Research Square

Preprints are preliminary reports that have not undergone peer review.
They should not be considered conclusive, used to inform clinical practice,
or referenced by the media as validated information.

Functional Validation of the Glucose Dehydrogenase Gene HaGDH in Harmonia axyridis

Ziliang Zheng
Guiyang University
Binkai Ma
Guiyang University
Xuyu Ran
Guiyang University
Mengmeng Zhao
Guiyang University
Dongmo Yang
Guiyang University
Xiujian Xiang
Guiyang University
Jiaxin Sun
Guiyang University
Guoyong Li
ligy0925@163.com
Guiyang University

Research Article

Keywords: Harmonia axyridis, Glucose dehydrogenase, Gene cloning, Expression analysis, Glucose content variation, RNA interference

Posted Date: October 26th, 2026

DOI: https://doi.org/10.21203/rs.3.rs-11343010/v1

License: This work is licensed under a Creative Commons Attribution 4.0 International License.
Read Full License

Additional Declarations: No competing interests reported.

Abstract

Background

As a vital natural enemy in farmland ecosystems, *Harmonia axyridis* plays an essential role in biological pest control. Glyphosate can be transmitted through the food chain, disrupting reproduction and diminishing the biocontrol performance of natural enemy.

Methods and Results

In this study, we cloned and characterized *HaGDH* (GenBank accession no. PZ594815.1), a key gene encoding glucose dehydrogenase involved in energy metabolism, and assessed its potential as a molecular target for natural enemy protection via RNA interference. The full-length transcript is 1920 bp, containing an 1869 bp coding sequence that encodes 622 amino acids. Phylogenetic analysis showed that *HaGDH* formed a monophyletic clade with GDH from *Coccinella septempunctata*, indicating the closest evolutionary relationship. *HaGDH* expression level in larvae was significantly higher than in pupae and adults, and its transcript abundance in elytra was approximately 6-fold higher than that in legs, consistent with the high energy demand for elytral cuticle development and maintenance. Upon exposure to 5 mg/L glyphosate, *HaGDH* expression reached 3.88 times that of the control, while it decreased to 0.60 times that of the control under 20 mg/L treatment. RNAi effectively silenced *HaGDH*, with nearly 50% reduction in gene expression at 24 h post-injection in 4th-instar larvae. Silencing of *HaGDH* reduced the 10-day larval survival rate to less than 10%.

Conclusion

These findings suggest that *HaGDH* can serve as a candidate molecular biomarker for evaluating the physiological toxicity of glyphosate to natural enemy, providing a molecular basis for natural enemy conservation and biological pest control.

Introduction

Harmonia axyridis, a holometabolous insect of the class Insecta, order Coleoptera, family Coccinellidae, serves as a pivotal natural enemy in the biological control of agricultural and forestry pests, and plays an irreplaceable role in maintaining ecological balance and reducing chemical pesticide application [1]. Glyphosate exerts its herbicidal activity by inhibiting 5-enolpyruvylshikimate-3-phosphate synthase (EPSPS), the key enzyme in the shikimic acid metabolic pathway of plants and microorganisms. Since the shikimic acid pathway is absent in insects, it has long been a prevailing academic consensus that glyphosate has no toxic side effects on insects and other animals [2, 3].However, accumulating evidence has confirmed that glyphosate can directly disrupt the survival and development of insects, which is of great significance for insect conservation and the management of non-target effects of pesticides [4; 5].

Furthermore, this toxic effect can be transferred to predatory natural enemy along the food chain. In *H. axyridis*, glyphosate exposure has been verified to disturb intestinal symbiotic microbiota, suppress growth, reduce body weight, and further impair its energy metabolism and reproductive capacity [6, 7].

Glucose dehydrogenase *(GDH*) is present in microorganisms, plants and animal cells. It participates in cellular energy metabolism and biosynthetic processes, and plays a critical role in maintaining redox homeostasis [8, 9]. In microorganisms, *GDH* has also evolved diverse specialized physiological functions; for example, a novel GDH involved in mineral weathering has been identified in *Collimonas pratensis* [10]. *GDH* is a member of the glucose-methanol-choline (*GMC*) oxidoreductase superfamily, a class of FAD-dependent enzymes. This superfamily was first formally defined by Cavener in 1992 based on sequence homology, and its classification framework and structural characteristics were further refined by subsequent large-scale evolutionary analyses [8, 11]. Members of the *GMC* family share a conserved structural architecture, comprising an N-terminal FAD-binding domain and a C-terminal substrate-binding domain, and maintain catalytic center function through a conserved catalytic histidine residue. Meanwhile, *GMC* family genes in insects universally exhibit developmental stage-specific expression profiles with well-defined functional differentiation [8, 9, 12]. Energy metabolism serves as the core physiological basis regulating the growth, development, reproductive capacity and environmental adaptability of *H. axyridis*, and carbohydrate uptake as well as the activity of metabolic pathways directly determine its developmental rate and oviposition potential [13]. Current studies on carbohydrate metabolism in *H. axyridis* mainly focus on the trehalose pathway. Two novel soluble trehalase genes, *Treh1-3* and *Treh1-4*, have been cloned and identified, confirming that trehalose and glycogen metabolism play critical roles in the regulation of cold tolerance under both short- and long-term cold stress. Low temperature can significantly upregulate the expression of the trehalose-6-phosphate synthase gene *TPS* and the trehalase gene *Treh1*, and enhance cold tolerance by promoting trehalose synthesis and metabolism. Among them, the *HaTPS* gene has been verified to exert a core regulatory role in the cold stress response of *H. axyridis* [14]. In addition, the expression regulation of the pyruvate kinase gene *PYK* can simultaneously affect glucose and trehalose metabolism, thereby modulating the reproductive capacity of *H. axyridis* [15]. Studies on other insect species have revealed that the catalytic activity of GDH is positively correlated with the hydrophobicity of its active pocket; specifically, the P45A mutant generated via site-directed mutagenesis shows an approximately 29-fold elevation in enzymatic activity [16]. In *Bombyx mori*, glucose-6-phosphate dehydrogenase (G6PDH) activity fluctuates dynamically throughout diapause and embryonic development, and is involved in maintaining redox homeostasis and mediating physiological adaptation under adverse conditions [17]. In *Laodelphax striatellus*, the *GDH* gene acts as the core mediator underlying validamycin-induced suppression of population reproduction. Following validamycin treatment, *GDH* expression is significantly downregulated, which leads to disrupted lipid synthesis, abnormal ovarian development and a substantial decline in fecundity [18]. In rice pest insects, *GMC* family genes mitigate high-temperature oxidative damage by enhancing antioxidant enzyme activity, thus improving their adaptability to high-temperature environments [19]. Additionally, *GMC* family members exhibit marked expression responses

under pesticide stress and feature conserved stress regulatory patterns across different insect orders, rendering them potential molecular targets for pesticide toxicity assessment [19, 20]. Despite substantial progress in research on *GDH* and the *GMC* superfamily in model and economically important insects, the interaction mechanisms of *GDH*-mediated signaling pathways, regulatory networks under multiple stress conditions, and application pathways for protein engineering strategies including site-directed mutagenesis and heterologous expression remain to be systematically and thoroughly elucidated in predatory insects such as ladybeetles.

As a core member of the GMC oxidoreductase superfamily, glucose dehydrogenase (GDH) has evolved diverse physiological functions across different insect taxa, including energy metabolism and chemical defense. In Coleoptera, the *GMC* oxidoreductase family exhibits remarkable functional diversification. Leaf beetle larvae drive the evolution of their larval chemical defense systems through independently recruited *GMC* family oxidases, ensuring their adaptation to host plant secondary metabolites and natural enemies [21]. In the bombardier beetle *Brachinus crepitans*, *GDH* expressed in defensive storage reservoirs can reversibly reduce toxic benzoquinones, preventing toxin accumulation and maintaining the homeostasis of the defense system [22]. In predatory ladybeetles such as *H. axyridis*, *GLUT*-mediated crosstalk between glucose and trehalose metabolism participates in the regulation of growth, development and stress responses [15]. In the *Tribolium castaneum* genome, tandemly duplicated *GMC* gene clusters have undergone duplication and functional divergence, driving the functional diversification of *GDH* [9]. Studies on dipteran *Drosophila* have confirmed that *GDH* is specifically localized to the female spermathecal ducts. Silencing of *GDH* significantly disrupts sperm storage and transport, resulting in disordered sperm distribution and prolonged oviposition cycles. In addition, *Drosophila GDH* exhibits a biphasic developmental expression pattern and is regulated by ecdysone to participate in cuticle development [12, 23, 24]. In the lepidopteran *Bombyx mori*, long-term domestication pressure has driven sequence variations in multiple *GMC* family genes, making these genes candidate targets for green management of lepidopteran pests [25]. Although basic research on *GDH* has been accumulated in Coleoptera, Diptera and Lepidoptera, systematic reports on the molecular identification and functional validation of the *HaGDH* gene in *H. axyridis* remain unavailable to date.

Accordingly, in this study, based on our previous transcriptome sequencing dataset of *H. axyridis* and integrated bioinformatic analyses, we obtained the full-length clone of the glucose dehydrogenase gene *HaGDH*, characterized its molecular properties, and elucidated its phylogenetic relationships. We further applied quantitative real-time PCR (RT-qPCR) to systematically profile the spatiotemporal expression patterns of *HaGDH* across different developmental stages and tissues of *H. axyridis*, as well as its transcriptional responses to gradient concentrations of glyphosate stress. Finally, targeted silencing of *HaGDH* was performed via RNA interference (RNAi). We verified the gene silencing efficiency and measured changes in glucose (Glc) content, to clarify the biological function of *HaGDH* in the regulation of energy metabolism and glyphosate stress response in *H. axyridis*. This study aims to screen candidate molecular markers for pesticide toxicity assessment in natural enemy, and provide a theoretical basis for the protection of beneficial field ladybeetle populations and the ecological risk evaluation of pesticides.

Materials and Methods

Insect

- The broad bean (*Vicia faba*) cultivar ‘Baipi’ used in this study was sourced from Yunnan Province, China. Seeds were soaked in warm water overnight. Vermiculite and nutrient soil were mixed thoroughly at a 2:1 volume ratio, then spread evenly into seedling trays (40 cm × 15 cm × 10 cm) to a thickness of approximately 3 cm. The pre-soaked seeds were placed on the surface of the growing medium and covered with a 3–5 mm thick layer of vermiculite. Each tray was sown with 25 seeds and watered to saturation immediately after sowing. The seedling trays were then transferred to a controlled climate chamber set to 25 ± 1°C, 70 ± 5% relative humidity, and a 14:10 h light:dark (L:D) photoperiod. Plants were watered every 2 days. When seedlings reached the three-leaf stage, their apical buds were removed, and the plants were subsequently infested with aphids. Throughout the experiment, 2–3 trays of broad bean seedlings were sown daily to maintain a steady, rotating supply of fresh host plants [15].
- Adults of the pea aphid (*Acyrthosiphon pisum*) and *H. axyridis* were collected in June 2026 from the Botanical Garden of Guiyang University, Guiyang, Guizhou Province, China (106.78° E, 26.56° N). All field-collected specimens were transferred to the Guizhou Provincial Key Laboratory of Agricultural Biosecurity and reared in controlled climate chambers under conditions of 25 ± 1°C, 70 ± 5% relative humidity and a 14:10 h light:dark (L:D) photoperiod. *A. pisum* was maintained on fresh broad bean seedlings, and *H. axyridis* was fed with *A. pisum*. Insects were reared for 5 consecutive generations prior to use in subsequent experiments [26].
- Samples of *H. axyridis* were collected across different developmental stages, including eggs, 1st–4th instar (L1–L4) larvae, pupae, female adults and male adults. For tissue-specific sampling, 4th-instar larvae were dissected under a stereomicroscope on ice, and eight tissue types were isolated: head, antennae, compound eyes, Malpighian tubules, thorax, legs, elytra and epidermis. For the glyphosate stress treatment assay, two test concentrations (5 mg/L and 20 mg/L) were prepared by diluting glyphosate with distilled water, with reference to previously reported sublethal concentrations of glyphosate in ladybeetles [27]. A 0 mg/L group treated with distilled water was set as the blank control. The immersion method was applied for larval exposure: healthy 4th-instar larvae with uniform developmental status were immersed in the corresponding solutions for 15 s, then air-dried and reared under standard conditions for 24 h. Subsequently, 10 surviving 4th-instar larvae were randomly selected from each treatment for subsequent analyses. Three biological replicates were established for each treatment. All collected samples were immediately stored in an ultra-low temperature freezer at − 80°C until further use.

Total RNA extraction and cDNA synthesis

- Total RNA was isolated from healthy 4th-instar larvae of *H. axyridis* using Trizol reagent. The integrity, purity and concentration of the extracted RNA were assessed via 1% agarose gel electrophoresis and spectrophotometry (NanoDrop ND-1000, USA), respectively. First-strand cDNA

was synthesized by reverse transcription using the EasyScript® One-Step gDNA Removal and cDNA Synthesis SuperMix kit (TransGen Biotech). The resulting products were stored at − 20°C for subsequent experiments.

Cloning of *HaGDH* from *H. axyridis*

Primers targeting *HaGDH* were designed using Primer Premier 5.0 (Table 1), based on the conserved regions of *GDH* genes in Coleoptera and the *H. axyridis* transcriptome dataset obtained previously by our research group. PCR amplification was performed in a 50 μL reaction system using cDNA from 4th-instar *H. axyridis* larvae as the template. The reaction mixture contained 25 μL of 2× Rapid Taq Master Mix, 2 μL of cDNA, 2 μL of each primer (10 μM), and nuclease-free water to adjust the final volume to 50 μL. The amplification protocol was set as follows: initial denaturation at 95°C for 5 min; followed by 34 cycles of denaturation at 95°C for 30 s, annealing at 50°C for 30 s, and extension at 72°C for 2 min; with a final extension step at 72°C for 10 min. After verification by 1% agarose gel electrophoresis, the target PCR bands were excised and purified using the HiPure Gel Pure DNA Mini Kit (Magen Biotech, Shanghai, China). The purified fragments were ligated into the pMD™18-T vector (TaKaRa) and subsequently transformed into DH5α competent cells. The transformation products were spread onto LB agar plates supplemented with ampicillin and incubated overnight at 37°C for 16 h. White single colonies were selected and identified by colony PCR. Positive clones were inoculated into ampicillin-containing LB liquid medium and cultured at 37°C with shaking at 200 rpm. The resulting bacterial suspensions were sent to Sangon Biotech (Shanghai) Co., Ltd. for sequencing.

Table 1
Primers for cloning of *HaGDH* Gene

Primers	Primer sequences(5' - 3')	Purpose
HaGDH-F	AGGCTTCGTTGTTGATGA	Full-length sequence amplification
HaGDH-R	GAGGTACACTTGGGTTTC	
q*HaGDH*-F	CTTGAAAGAGGCGGAGAC	Target gene amplification in real-time quantitative PCR
q*HaGDH*-R	CAATAAGGGTGAGAACAT	
ds-*HaGDH*-F	GGAACTTTGGTTGGATTG	dsRNA synthesis
T-ds-*HaGDH*-F	ggatcctaatacgactcactataggGGAACTTTGGTTGGATTG	
ds-*HaGDH*-R	GGGTTTTTGTTAGGTATG	
T-ds-*HaGDH*-R	ggatcctaatacgactcactataggGGGTTTTTGTTAGGTATG	
q*HaRP*49-F	GCGATCGCTATGGAAAACTC	Reference gene amplification in real-time quantitative PCR
q*HaRP49*-R	TACGATTTTGCATCAACAGT	

Bioinformatics analysis

- Details of the software packages and analytical items applied for bioinformatic analysis are summarized in Table 2. Multiple sequence alignment of HaGDH with homologous proteins from 12 insect species was conducted using ClustalW. Thirty-one species with high amino acid sequence homology to HaGDH were screened and retrieved from the NCBI database (Table 3).

Table 2
Bioinformatics software and tools used in this study

The name of the software	The analysis project	Website
ORF finder	Open reading frame search	https://www.ncbi.nlm.nih.gov/gorf/gorf.html
Protparam	Analysis of physical and chemical properties of proteins	https://www.expasy.org/resources/protparam
Protscale	The prediction of protein hydrophilicity distribution	https://www.expasy.org/resources/protscale
TMHMM	The prediction of protein transmembrane structure	https://services.healthtech.dtu.dk/services/TMHMM/
SignalP 6.0	The prediction of protein signal	https://www.cbs.dtu.dk/services/SignalP/
NetPhos3.1	Protein phosphorylation site prediction	https://services.healthtech.dtu.dk/services/NetPhos/
PSORT	Protein subcellular localization	https://www.genscript.com/psort.html
SOPMA	Prediction of protein secondary structure	https://npsa-prabi.ibcp.fr
SWISS-MODEL	Prediction of protein three-dimensional structure	https://swissmodel.expasy.org/
PyMOL	Edit and output 3D structure	https://www.pymli.org/
NCBI	Search gene sequence	https://blast.ncbi.nlm.nih.gov/Blast.cgi
ClustalW	Homology comparison of gene sequences was performed	https://www.ebi.ac.uk/clustalw/
MEGA-X	Phylogenetic tree construct(p-distance, Bootstrap = 1000)	https://www.megasoftware.net
Note: all analyses are computational predictions from sequences.		

Table 3
Information of the insect species for phylogenetic analysis.

Genus	Species and the type of GDH	GenBank accession numbers from NCBI
Coleoptera	*Harmonia axyridis* GDH	PZ594815.1
	Coccinella septempunctata GDH	XP_044763975.1
	Diabrotica virgifera GDH	XP_028134088.1
	Diorhabda carinulata GDH	XP_057669065.1
	Anoplophora glabripennis GDH	XP_018569543.1
	Leptinotarsa decemlineata GDH	XP_074030305.1
	Anthonomus grandis GDH	XP_050302397.1
	Rhynchophorus ferrugineus GDH	XP_076256267.1
	Aethina tumida GDH	XP_019869157.2
	Zophobas morio GDH	XP_063930047.1
	Tenebrio molitor GDH	XP_068900342.1
	Tribolium madens GDH	XP_044261107.1
	Tribolium castaneum GDH	XP_972430.2
Hymenoptera	*Neodiprion fabricii* GDH	XP_046414137.1
	Neodiprion lecontei GDH	XP_015512604.1
	Diprion similis GDH	XP_046753934.1
	Athalia rosae GDH	XP_048505703.1
	Colletes gigas GDH	XP_043257484.1
	Hylaeus anthracinus GDH	XP_054004403.1
	Nomia melanderi GDH	XP_031838213.1
	Dufourea novaeangliae GDH	XP_015431032.1
Diptera	*Topomyia yanbarensis* GDH	XP_058821937.1
	Culex quinquefasciatus GDH	XP_038122031.1
	Culex pipiens pallens GDH	XP_039446506.1
	Ochlerotatus camptorhynchus GDH	XP_065093139.1
	Aedes aegypti GDH	XP_021710641.1

Genus	Species and the type of GDH	GenBank accession numbers from NCBI
	Aedes albopictus GDH	XP_062711440.1
Lepidoptera Outgroup	*Bicyclus anynana* GDH	XP_023937296.2
	Aricia agestis GDH	XP_041972116.1
	Trichoplusia ni GDH	XP_026735685.1
	Helicoverpa zea GDH	XP_047036442.1

RT-qPCR analysis

The relative transcript levels of *HaGDH* in *H. axyridis* across different developmental stages, tissue types and graded concentrations of glyphosate were quantified by quantitative real-time PCR (RT-qPCR). The ribosomal protein gene *HaRP49* was selected as the endogenous reference gene, and *HaGDH*-specific primers were designed using Primer Premier 5.0 (Table 1). PCR amplification was carried out according to the manufacturer's protocol of the TB Green® Premix DimerEraser™ kit (TaKaRa). The 20 μL reaction mixture consisted of 1 μL of cDNA template, 10 μL of 2× TB Green Premix DimerEraser, 0.4 μL of each forward and reverse primer, and ddH_2O to adjust the final volume to 20 μL. Three biological replicates were established for each assay. The amplification protocol comprised an initial denaturation step at 95°C for 5 min, followed by 40 cycles of denaturation at 95°C for 5 s and combined annealing/extension at 60°C for 40 s.

- dsRNA synthesis
- *In vitro* synthesis of ds*HaGDH* was performed using the T7 RiboMAX™ Express RNAi System kit (Promega, Madison, WI, USA), with primer details listed in Table 1. Following verification via 1% agarose gel electrophoresis, the synthesized dsRNA was diluted to a final concentration of 500 ng/μL with nuclease-free water and stored at − 80°C until use. Healthy 4th-instar larvae with uniform body size and developmental status were selected for the RNAi assay. A volume of 250 nL of ds*HaGDH* was injected into the ventral intersegmental membrane between the second and third abdominal segments from the posterior end, using a microinjector (Nanoliter 2010, USA). Coleopteran insects generally exhibit high RNAi sensitivity to dsRNA delivered via microinjection [28]; therefore, microinjection was employed as the dsRNA delivery method in this study. Larvae in the control group were injected with an equivalent volume of ds*GFP*. Each treatment contained 15 individuals. Two experimental groups were set up. The first group was used to assess RNAi silencing efficiency and larval survival. Samples were collected at 24, 48 and 72 h post-injection and immediately frozen at − 80°C. Total RNA extraction and cDNA synthesis were conducted according to the procedure described in the Total RNA extraction and cDNA synthesis section, and RT-qPCR was performed as described in Section 1.5 to quantify the silencing efficiency at each time point. Meanwhile, larval mortality was monitored and recorded daily for 10 days after injection. The second group was used for glucose content determination. The whole-body glucose content of

larvae sampled at 24, 48 and 72 h post-injection was measured using a glucose content assay kit (BOXBIO, Beijing, China) [29]. All treatments were established with three independent biological replicates.

Data analysis

Raw experimental data were collated and processed using Microsoft Excel 2024. Statistical analyses were performed using IBM SPSS Statistics 27.0 (SPSS Inc., Chicago, IL, USA). One-way analysis of variance (ANOVA) was applied, followed by Tukey's post hoc test for multiple comparisons. The relative expression levels of target genes and the silencing efficiency of *HaGDH* upon RNAi treatment were calculated using the $2^{-\Delta\Delta Ct}$ method [30]. All data are presented as mean ± standard error (SE). Differences were considered statistically significant at $p \leq 0.05$ and highly significant at $p \leq 0.001$. Finally, data visualization and graph generation were completed using GraphPad Prism 10.6 software.

Results

Cloning and sequence analysis of *HaGDH*

The glucose dehydrogenase gene was successfully cloned from *H. axyridis* and designated *HaGDH* (GenBank accession number: PZ594815.1). The full-length transcript of *HaGDH* is 1920 bp, containing an open reading frame (ORF) of 1869 bp that encodes 622 amino acids. Domain analysis indicated that the HaGDH protein possesses the characteristic conserved domains of the GMC superfamily: a GMC_oxred_N domain spanning residues 56 to 354 at the N-terminus, and a GMC_oxred_C domain spanning residues 465 to 609 at the C-terminus. GMC stands for glucose-methanol-choline oxidoreductase, a superfamily of FAD-dependent oxidoreductases, and glucose dehydrogenase is a canonical member of this superfamily (Fig. 1). Physicochemical property predictions revealed that the HaGDH protein has a molecular formula of $C_{3099}H_{4852}N_{844}O_{893}S_{23}$, with a relative molecular mass of 68.96 kDa and a theoretical isoelectric point (pI) of 8.98, classifying it as a basic protein. It contains 58 negatively charged amino acid residues and 67 positively charged amino acid residues. The extinction coefficient of HaGDH is 96635, and its instability index is 36.92, which is below the general threshold of 40 for stable proteins, confirming HaGDH as a structurally stable protein. The aliphatic index is 87.59, and the grand average of hydropathicity (GRAVY) is − 0.161 (Table 4). Hydrophobicity analysis showed that the overall amino acid sequence of HaGDH is hydrophilic (Fig. S1). In addition, HaGDH contains multiple phosphorylation sites located on tyrosine, threonine and serine residues (Fig. S2). Subcellular localization prediction indicated that the protein is predominantly distributed in mitochondria (30.40%) and cytoplasm (26.10%), followed by the nucleus and cell membrane (13.00% each), with a small fraction localized in vacuoles and the endoplasmic reticulum (8.75% each) (Fig. S3).

Table 4
Physical and chemical properties of HaGDH

Item	**HaGDH**
Protein molecular formula	$C_{3099}H_{4852}N_{844}O_{893}S_{23}$
Relative molecular mass(kDa)	68.96
Theoretical isoelectric point(pI)	8.98
Leu content(%)	8.7
Gly content(%)	8.5
Ser content(%)	7.6
Val content(%)	7.6
Ile content(%)	6.6
Pro content(%)	6.4
Thr content(%)	6.3
Ala content(%)	6.1
Arg content(%)	6.1
Asp content(%)	5.3
Lys content(%)	4.7
Asn content(%)	4.5
Glu content(%)	4.0
Phe content(%)	3.9
Tyr content(%)	3.9
Gln content(%)	2.6
Met content(%)	2.6
His content(%)	1.9
Trp content(%)	1.8
Cys content(%)	1.1
Total number of negatively charged residues	58
Total number of positively charged residues	67
Extinction coefficients	96635
Half-life(h)	30

Item	HaGDH
Instability index	36.92
Aliphatic index	87.59
Grand average of hydropathicity (GRAVY)	-0.161

Protein structure analysis of HaGDH

- Secondary structure prediction conducted via the online tool SOPMA indicated that the HaGDH protein is classified as an α/β protein. α-helices serve as the core structural elements, widely distributed across the full length of the protein and forming the main scaffold that supports its overall spatial folding. Meanwhile, multiple β-strands are arranged in the central core region, which can further assemble into β-sheets and contribute to the formation of the enzyme's coenzyme-binding pocket and catalytic active center. The remaining regions are interspersed and linked by random coils and flexible loop regions, which mediate the assembly of structural modules and conformational regulation. This secondary structure architecture is consistent with the canonical structural features of the GMC oxidoreductase family (Fig. 2a). Homology modeling of the tertiary structure of the HaGDH protein was performed using SWISS-MODEL, with a GMC oxidoreductase from *Rhynchophorus ferrugineus* (UniProt ID: A0A834HW68.1.A) as the template. The sequence identity between the two proteins was 79.32%. The global model quality estimate (GMQE) score of the resulting model was 0.93, which is well above the generally accepted reliability threshold for homology modeling (GMQE > 0.7), demonstrating excellent model quality. The tertiary structure also displayed the characteristic folding features of an α/β protein. The HaGDH protein adopts an overall monomeric globular conformation, assembled by extensive stacking of α-helices and multiple β-sheets, which form two functionally well-defined domains. The N-terminal region is built around a Rossmann fold core, in which α-helices wrap around the internal β-sheet layer to constitute the FAD coenzyme-binding domain. The C-terminal region likewise uses α-helices as the main scaffold, which together with β-strands form the active center responsible for substrate binding and catalysis. In addition, an independent long α-helix extends from the N-terminus of the protein, which is predicted to be a transmembrane anchoring region. This three-dimensional folding pattern is highly consistent with the canonical structure of the GMC oxidoreductase family, and corroborates the compositional features of the secondary structure (Fig. 2b).

Multiple sequence alignment and phylogenetic analysis

Sequence alignment was performed between the HaGDH protein of *H. axyridis* and GDH homologs from closely related coleopteran species spanning six families

Coccinellidae, Tenebrionidae, Nitidulidae, Chrysomelidae, Cerambycidae and Curculionidae. The selected species included *Coccinella septempunctata*, *Tribolium castaneum*, *Tenebrio molitor*, *Zophobas morio*,

Aethina tumida, *Diabrotica virgifera*, *Anoplophora glabripennis*, *Leptinotarsa decemlineata*, *Anthonomus grandis*, *Rhynchophorus ferrugineus* and *Diorhabda carinulata*. The alignment results demonstrated that the GDH proteins of these 12 insect species exhibited high sequence conservation at the C-terminal region (Fig. 3). Phylogenetic tree analysis showed that HaGDH from *H. axyridis* clustered into a single well-supported clade with *C. septempunctata* (Coccinellidae) with high bootstrap confidence, indicating the closest evolutionary relationship between the two. In contrast, this protein shared the most distant phylogenetic relationship with GDH from the lepidopteran species *Helicoverpa zea* (Fig. 4).

Expression analysis of *HaGDH* gene

- The expression pattern of *HaGDH* across developmental stages followed a trend of initial elevation followed by a subsequent decline. Transcript abundance reached its peak at the 2nd instar (L_2) larval stage, representing the absolute maximum value throughout the entire developmental cycle. Expression levels in eggs, pupae, male adults (M-A), female adults (F-A), and 1st (L_1), 3rd (L_3) and 4th (L_4) instar larvae were all significantly lower than those at the L_2 stage ($p \leq 0.05$) (Fig. 5a). Across different tissues, *HaGDH* showed the highest expression in elytra, with a relative expression level close to 3, whereas the lowest levels were found in legs and Malpighian tubules (approximately 0.5). The relative expression levels in antennae and thorax were also significantly lower than those in elytra (Fig. 5b). Glyphosate stress significantly modulated *HaGDH* expression (Fig. 5c). The 5 mg/L treatment induced the strongest upregulation, with the expression level approximately 3.88-fold that of the control group ($p \leq 0.001$). At the 20 mg/L concentration, however, the regulatory effect shifted from induction to inhibition: gene expression was significantly downregulated relative to the control, dropping to 0.60-fold of the control level.

Functional analysis of the *HaGDH* gene

RNA interference (RNAi) was employed to silence the *HaGDH* gene in *H. axyridis*, with ds*GFP* serving as the negative control. Gene transcript levels were detected at 24, 48 and 72 h post-injection. The results demonstrated that the silencing effect of *HaGDH* was time-dependent. At 24 h after ds*HaGDH* injection, the gene expression level decreased by approximately 50% relative to the control group. The silencing efficiency peaked at 48 h, when the transcript abundance dropped to the lowest level. At 72 h, the gene expression level showed a slight rebound compared with that at 48 h, but remained significantly lower than that of the control group (24 h: $p \leq 0.01$; 48 h and 72 h: $p \leq 0.001$). These findings indicated that the dsRNA could exert a stable and highly efficient silencing effect in larvae (Fig. 6a). Furthermore, the transcript level of *HaGDH* at 72 h showed a slight rebound compared with that at 48 h. Two potential mechanisms may account for this observation: first, dsRNA is gradually degraded by endogenous nucleases *in vivo*, leading to a decline in interference efficacy; second, the gene may partially restore its expression through compensatory upregulation at the transcriptional level. This underlying mechanism remains to be further verified in subsequent experiments. Survival rate statistics showed that only minor mortality occurred in the ds*GFP* control group within 10 days, with the survival rate remaining above 60%. In contrast, the survival rate of the ds*HaGDH* treatment group decreased continuously over time post-

injection, dropping to less than 10% by day 10, which was significantly lower than that of the control group (Fig. 6b). Determination of whole-body glucose content revealed that silencing *HaGDH* induced significant alterations in glucose homeostasis in *H. axyridis*. At all three detection time points (24, 48 and 72 h), the glucose content in the ds*HaGDH* treatment group was significantly lower than that in the ds*GFP* control group. The difference reached a highly significant level at 24 h and 48 h ($p \leq 0.01$), and became even more pronounced at 72 h ($p \leq 0.001$). The reducing effect on glucose content persisted with the extension of RNAi duration (Fig. 7). Under normal physiological conditions, *GDH* catalyzes glucose oxidation to supply energy. Theoretically, silencing *HaGDH* would block glucose consumption through this pathway and result in elevated intracellular glucose levels. However, a significant reduction in glucose content was observed in this study, contrary to the expected trend. It is speculated that silencing *HaGDH* triggers compensatory regulation of glucose metabolism in the insect: when the *GDH*-mediated glucose oxidation pathway is blocked, the insect may activate alternative glycolytic pathways to accelerate glucose utilization, thereby maintaining energy metabolism and redox homeostasis, which ultimately leads to the continuous depletion of glucose reserves.

Discussion

Glucose dehydrogenase (*GDH*), a canonical member of the *GMC* oxidoreductase superfamily, is a key functional protein that regulates energy metabolism and maintains redox homeostasis in insects. Its sequence conservation and functional diversification constitute one of the crucial molecular bases underlying insect adaptation to environmental stress. In this study, the *HaGDH* gene was cloned from *H. axyridis*. The encoded protein harbors two conserved domains, *GMC*_oxred_N and *GMC*_oxred_C, which is consistent with the typical structural features of *GMC* family proteins. Secondary and tertiary structure predictions revealed that HaGDH is a typical α/β protein, with α-helices forming the core scaffold and multiple β-strands assembled into sheet structures distributed across the polypeptide. The tertiary structure adopts an overall monomeric globular conformation: the N-terminus forms a FAD coenzyme-binding domain via a Rossmann fold, while the C-terminus constitutes the substrate-binding and catalytic active center. A predicted transmembrane anchoring helix also extends from the N-terminus. This folding pattern is highly consistent with GDH protein structures reported in other insect species such as *Tribolium castaneum* and *Drosophila* spp., further validating the family assignment and functional conservation of this gene [9]. Phylogenetic analysis showed that HaGDH clustered into the same clade with GDH from *Coccinella septempunctata* (Coccinellidae), indicating the closest phylogenetic relationship, whereas it shared the most distant relationship with lepidopteran GDH homologs. This evolutionary distribution pattern aligns with the traditional taxonomic status of insects, suggesting that GDH proteins have retained high sequence conservation during coleopteran evolution and their core catalytic function remains relatively stable. This finding is consistent with the conclusion regarding the long-term evolutionary conservation of the *GDH* gene in *Drosophila* [9, 31].

The spatiotemporal expression pattern of a gene serves as a critical basis for elucidating its physiological function. In this study, we found that *HaGDH* was expressed throughout the entire

developmental cycle of *H. axyridis*, with its expression peak occurring at the 2nd instar larval stage, which was significantly higher than the levels detected at the egg, pupal and adult stages. The larval stage represents the period of highest food intake and most rapid growth and development in *H. axyridis*, associated with the greatest demand for energy supply and biosynthesis. Highly expressed *GDH* can continuously supply ATP and reducing equivalents by catalyzing glucose oxidation and catabolism, thereby meeting the energy requirements of larval growth and metabolism. This finding is consistent with previous reports that *GDH* participates in cuticle development in *Drosophila* and that glucose-6-phosphate dehydrogenase in the silkworm (*Bombyx mori*) undergoes dynamic changes during embryonic development, suggesting that *GDH* exerts a conserved function in the regulation of insect developmental metabolism [12, 17]. This expression profile also aligns with the expression characteristics of the trehalase gene in *H. axyridis* during critical developmental stages [32]. Tissue expression analysis showed that *HaGDH* exhibited the highest expression level in elytra, and the expression level in the head was significantly higher than that in tissues such as the thorax and legs. As a characteristic protective structure of coleopteran insects, the development and structural maintenance of the elytral cuticle depend on robust energy metabolism and biosynthesis [33]; whereas the head, with its dense neural tissue, imposes higher demands on energy homeostasis and redox balance, thus requiring elevated *GDH* expression to support relevant physiological activities. This finding is consistent with previous reports of high expression of sugar metabolism genes in the head of *H. axyridis* [15]. Under glyphosate stress, *HaGDH* expression displayed a dose-response pattern characterized by induction at low concentrations and inhibition at high concentrations: after treatment with 5 mg/L glyphosate, the expression level was upregulated to 3.88-fold that of the control, whereas it decreased markedly at the high concentration of 20 mg/L. It is speculated that low-concentration glyphosate induces a metabolic compensatory response in insects: by upregulating *GDH* transcription, it enhances glucose metabolic flux and improves antioxidant capacity to alleviate oxidative damage caused by the pesticide. This stress regulatory pattern has been reported in insects under various adverse conditions such as high temperature and pesticide exposure [19, 34]; whereas the cytotoxicity of high-concentration glyphosate exceeds the compensatory regulatory capacity of the insect, directly inhibiting gene transcriptional activity and impairing metabolic function. This response pattern is consistent with the toxic effects of glyphosate on the energy metabolism system of non-target insects [4, 35]. A similar dynamic regulatory mechanism of *GDH* expression under stress has also been documented in other invertebrates such as the sea urchin *Strongylocentrotus intermedius*, where its expression can be directly mediated by upstream factors such as *HIF-1α* and participates in maintaining energy homeostasis under adverse conditions [36]. It has also been confirmed in *H. axyridis* that exposure to high-concentration glyphosate disrupts the intestinal symbiotic microbiota, reduces body weight and inhibits survival, exerting multi-dimensional disruptive effects on internal homeostasis and exhibiting typical dose-dependent toxicity characteristics [6, 27].

RNA interference results demonstrated that injection of ds*HaGDH* achieved efficient silencing of *HaGDH*, and the silencing effect exhibited distinct time-dependence: the gene expression level decreased by approximately 50% at 24 h, the silencing efficiency peaked at 48 h, and the expression level showed a slight rebound at 72 h. The rebound in expression may be attributed to two factors: on the one hand,

dsRNA is gradually degraded by endogenous nucleases *in vivo*, leading to a progressive reduction in interference efficacy; on the other hand, it suggests that the insect may partially restore gene expression through compensatory upregulation at the transcriptional level. This dynamic change is consistent with the general pattern of dsRNA interference in insects. Functional validation revealed that silencing of *HaGDH* caused a continuous decline in the survival rate of *H. axyridis*, with the survival rate dropping to less than 10% within 10 days. This indicates that *GDH* is a key gene for maintaining normal physiological activities in *H. axyridis* larvae, and its functional deficiency triggers severe physiological disorders and ultimately leads to individual mortality. This finding aligns with previous studies in the small brown planthopper (*Laodelphax striatellus*), where silencing of the *GDH* gene resulted in abnormal ovarian development and significantly reduced population fecundity, further confirming the core role of GDH in regulating insect survival and reproduction [18, 37]. Notably, the whole-body glucose content showed a continuous and significant decreasing trend after *HaGDH* silencing, which was contrary to the expectation based on the classic function of *GDH* in catalyzing glucose oxidation and catabolism [15]. It is speculated that when the *GDH*-mediated glucose oxidation pathway is blocked, the insect activates a compensatory regulatory mechanism of glucose metabolism: by activating alternative glucose catabolic pathways such as glycolysis and the pentose phosphate pathway, it accelerates the decomposition and utilization of glucose to maintain ATP supply and NADPH production, thereby preserving energy metabolism and redox balance, which ultimately leads to the continuous depletion of internal glucose reserves. Such compensatory remodeling of metabolic networks has been reported in previous studies on silencing of sugar metabolism genes in insects, and also indirectly explains the intrinsic mechanism underlying the high mortality of test insects after *HaGDH* silencing [15, 29]. This also further validates that *GMC* family genes can serve as reliable molecular markers for the evaluation of pesticide non-target toxicity, which is highly consistent with the expression profiles of GMC family genes in response to pesticide stress in lepidopteran insects [20].

Conclusions

- In this study, by integrating gene cloning, bioinformatic analysis and RNAi technology, we characterized the molecular features of the glucose dehydrogenase gene *HaGDH* from *H. axyridis*. The full-length transcript is 1920 bp, containing an open reading frame (ORF) of 1869 bp that encodes 622 amino acids. Glyphosate stress significantly modulated *HaGDH* expression, and gene silencing led to decreased glucose content and a sharp decline in survival rate in the insects, confirming that *HaGDH* exerts important functions in energy metabolism and adverse stress response in *H. axyridis*. These findings indicate that *HaGDH* can serve as a candidate molecular marker for assessing the physiological toxicity of pesticides, providing theoretical support for the protection of *H. axyridis* as a natural enemy and the ecological risk assessment of pesticides. Nevertheless, the specific mechanism underlying the synergistic regulation of energy metabolism by members of the *GMC* oxidoreductase family remains to be further explored.

Abbreviations

- ANOVA Analysis of Variance
- Ant Antenna
- bp Base pair
- cDNA complementary DNA
- CE Compound eye
- Cu Cuticle
- ddH_2O double distilled water
- dsRNA double-stranded RNA
- Ely Elytron
- EPSPS 5-enolpyruvylshikimate-3-phosphate synthase
- F-A Female adult
- FAD flavin adenine dinucleotide
- G6PDH Glucose-6-phosphate dehydrogenase
- GDH Glucose dehydrogenase
- GFP Green fluorescent protein
- Glc Glucose
- GLUT Glucose Transporter
- GMC Glucose-methanol-choline
- GMQE global model quality estimate
- GRAVY grand average of hydropathicity
- H. axyridis Harmonia axyridis
- HaGDH Harmonia axyridis glucose dehydrogenase
- HaRP49 Harmonia axyridis ribosomal protein 49
- Hd Head
- HIF-1α Hypoxia-Inducible Factor 1-alpha
- kDa Kilodalton
- L1 1st instar larva
- L2 2nd instar larva
- L3 3rd instar larva
- L4 4th instar larva
- LB Luria-Bertani medium
- L:D Light:Dark
- M-A Male adult
- Mp Malpighian tubules

- NCBI National Center for Biotechnology Information
- ORF Open Reading Frame
- P Pupa
- PCR Polymerase chain reaction
- pI Isoelectric point
- PYK Pyruvate kinase
- RNAi RNA interference
- RT-qPCR Quantitative real-time PCR
- SE Standard error
- SPSS Statistical Package for the Social Sciences
- Th Thorax
- TPS Trehalose-6-phosphate synthase

Declarations

Acknowledgements

The authors acknowledge the respected reviewers for the recommendations to improve our manuscript.

Author contributions

Ziliang Zheng Writing – review & editing, Conceptualization, Data curation, Validation, Resources, Methodology, Investigation. Binkai Ma, Writing – original draft, Validation, Resources, Methodology, Investigation. Xuyu Ran, Writing – original draft, Conceptualization, Methodology. Mengmeng Zhao, Conceptualization, Methodology. Dongmo Yang, Conceptualization, Methodology. Xiujain Xiang, Conceptualization, Methodology. Jiaxin Sun, Conceptualization, Methodology. Guoyong Li, Supervision, Project administration, Funding acquisition, Conceptualization.

Funding

The present study was supported by the Guizhou Provincial Basic Research Program (Natural Science) (QKHJC-ZK[2023]-019), the Guizhou Key Laboratory of Agricultural Biosecurity (ZSYS[2025]024), and the Innovative high-level talents project in Guizhou Province (GCC[2023]021).

Data availability

All the data analysed during this study are included in the manuscript. An additional set of figure is provided in supplementary files.

Declarations competing interest

The authors declare no competing interests.

References

1. Koch RL (2003) The multicolored Asian lady beetle, *Harmonia axyridis*: A review of its biology, uses in biological control, and non-target impacts. J Insect Sci 3(1):32. https://doi.org/10.1673/031.003.3201
2. Stork NE (2018) How many species of insects and other terrestrial arthropods are there on earth? Ann Rev Entomol 63:31–45. https://doi.org/10.1146/annurev-ento-020117-043348
3. Vicini JL, Reeves WR, Swarthout JT, Karberg KA (2019) Glyphosate in livestock: feed residues and animal health. J Anim Sci 97(11):4509–4518. https://doi.org/10.1093/jas/skz295
4. Vázquez DE, Ilina N, Pagano EA, Zavala JA, Farina WM (2018) Glyphosate affects the larval development of honey bees depending on the susceptibility of colonies. PLoS ONE 13(10):e0205074. https://doi.org/10.1371/journal.pone.0205074
5. Smith DFQ, Camacho E, Thakur R, Barron AJ, Casadevall A (2021) Glyphosate inhibits melanization and increases susceptibility to infection in insects. PLoS Biol 19(5):e3001182. https://doi.org/10.1371/journal.pbio.3001182
6. Gao XK, Hu FM, Zhang S, Luo JY, Zhu XZ, Wang L, Zhang KX, Li DY, Ji JC, Niu L, Wu CC, Cui JJ (2021) Glyphosate exposure disturbs the bacterial endosymbiont community and reduces body weight of the predatory ladybird beetle *Harmonia axyridis* (Coleoptera: Coccinellidae). Sci Total Environ 790:147847. https://doi.org/10.1016/j.scitotenv.2021.147847
7. Su ZH, Xu WY, Fu LY, Liu DY, Yan XY, Chen Y, Wang YC, Liu CX (2026) Sublethal effects of field-recommended glyphosate exposure on the predatory insect *Arma chinensis*: Growth inhibition and reproductive costs. Environ Pollut 389:128702. https://doi.org/10.1016/j.envpol.2026.128702
8. Sützl L, Foley G, Gillam EMJ, Bodén M, Haltrich D (2019) The GMC superfamily of oxidoreductases revisited: analysis and evolution of fungal GMC oxidoreductases. Biotechnol Biofuels 12:118. https://doi.org/10.1186/s13068-019-1457-0
9. Iida K, Cox-Foster DL, Yang X, Ko WY, Cavener DR (2007) Expansion and evolution of insect GMC oxidoreductases. BMC Evol Biol 7(1):75. https://doi.org/10.1186/1471-2148-7-75
10. Picard L, Turpault MP, Oger PM, Uroz S (2020) Identification of a novel type of glucose dehydrogenase involved in the mineral weathering ability of *Collimonas pratensis* strain PMB3(1). FEMS Microbiol Ecol 96(11):fiaa232. https://doi.org/10.1093/femsec/fiaa232
11. Cavener DR (1992) GMC oxidoreductases. A newly defined family of homologous proteins with diverse catalytic activities. J Mol Biol 223(3):811–814. https://doi.org/10.1016/0022-2836(92)90992-S
12. Cox-Foster DL, Schonbaum CP, Murtha MT, Cavener DR (1990) Developmental expression of the glucose dehydrogenase gene in *Drosophila melanogaster*. Genetics 124(4):873–880. https://doi.org/10.1093/genetics/124.4.873

13. Li Y, Wang SS, Liu YK, Lu YT, Zhou M, Wang S, Wang SG (2020) The effect of different dietary sugars on the development and fecundity of *Harmonia axyridis*. Front Physiol 11:574851. https://doi.org/10.3389/fphys.2020.574851
14. Qin Z, Wang S, Wei P, Xu CD, Tang B, Zhang F (2012) Molecular cloning and cold-induced expression of trehalose-6-phosphate synthase gene in *Harmonia axyridis* (Coleoptera: Coccinellidae). Acta Entomologica Sinica 55(6):651–658. https://doi.org/10.16380/j.kcxb.2012.06.014
15. Ge XZ, Shi YX, Wang SS, Liu ZH, Cai WJ, Zhou M, Wang SG, Tang B (2021) Sequence analysis of *Harmonia axyridis* pyruvate kinase gene and its regulation of trehalose metabolism. Scientia Agricultura Sinica 54(23):5021–5031. https://doi.org/10.3864/j.issn.0578-1752.2021.23.008
16. Li H, Bao QQ, Zhao JF, Xu YB, Yang SY, Xue WS, Sun Y, Liu YP (2022) Directed evolution engineering to improve activity of glucose dehydrogenase by increasing pocket hydrophobicity. Front Microbiol 13:1044226. https://doi.org/10.3389/fmicb.2022.1044226
17. Ghani MU, Yang ZH, Feng TX, Chen JF, Khosravi ZH, Wu QS, Cui HJ (2024) Comprehensive review on glucose 6 phosphate dehydrogenase: A critical immunometabolic and redox switch in insects. Int J Biol Macromol PP132867. https://doi.org/10.1016/j.ijbiomac.2024.132867
18. Ding J, Wu Y, You LL, Xu B, Ge LQ, Yang GQ, Wu JC (2017) Jinggangmycin-suppressed reproduction in the small brown planthopper (SBPH), *Laodelphax striatellus* (Fallén), is mediated by glucose dehydrogenase (GDH). Pestic Biochem Physiol 139:73–78. https://doi.org/10.1016/j.pestbp.2017.05.003
19. Quan PQ, Li JR, Liu XD (2023) Glucose dehydrogenases-mediated acclimation of an important rice pest to global warming. Int J Mol Sci 24(12):10146. https://doi.org/10.3390/ijms241210146
20. Xiao CH, Quan PQ, Zhu J, Lei HX, Li KL, Zhao X, Zhu DH, Zeng Y, Ma MY (2025) Identification and analysis of the GMC oxidoreductase family genes in *Cnaphalocrocis medinalis* and their response to spinetoram. Insects 16(12):1272. https://doi.org/10.3390/insects16121272
21. Rahfeld P, Kirsch R, Kugel S, Wielsch N, Stock M, Groth M, Boland W, Burse A (2014) Independently recruited oxidases from the glucose-methanol-choline oxidoreductase family enabled chemical defences in leaf beetle larvae (subtribe Chrysomelina) to evolve. Proceedings of the Royal Society B: Biological Sciences 281(1788): 20132921. https://doi.org/10.1098/rspb.2013.2921
22. Vogel H, Rügen N, Wielsch N, Twyman RM, Tonk-Rügen M, Vilcinskas A (2025) Molecular basis of the explosive defence response in the bombardier beetle *Brachinus crepitans*. Royal Soc Open Sci 12(5):241823. https://doi.org/10.1098/rsos.241823
23. Iida K, Cavener DR (2004) Glucose dehydrogenase is required for normal sperm storage and utilization in female *Drosophila melanogaster*. J Exp Biol 207(4):675–681. https://doi.org/10.1242/jeb.00816
24. Cavener DR, MacIntyre RJ (1983) Biphasic expression and function of glucose dehydrogenase in *Drosophila melanogaster*. Proc Natl Acad Sci USA 80(20):6286–6288. https://doi.org/10.1073/pnas.80.20.6286

25. Cheng DJ, Tang L, Meng M, Wang YH, Xia QY (2014) Sequence Variation of Two GMC Oxidoreductase Genes with Selective Signals Behind Silkworm Domestication. Acta Sericologica Sinica 40(2):210–215. https://doi.org/10.13441/j.cnki.cykx.2014.02.006
26. Li GY, Liu MK, Zheng ZL, Yang ZL, Liu YY, Li C, Smagghe G (2026) From plant to predator: glyphosate trophic transfer harms ladybird physiology and reproduction. Pest Manag Sci 82(6):5515–5527. https://doi.org/10.1002/ps.70656
27. Gao XK, Hu FM, Cui HF, Zhu XZ, Wang L, Zhang KX, Li DY, Ji JC, Luo JY, Cui JJ (2023) Glyphosate decreases survival, increases fecundity, and alters the microbiome of the natural predator *Harmonia axyridis* (ladybird beetle). Environ Res 238:117174. https://doi.org/10.1016/j.envres.2023.117174
28. Zhu KY, Palli SR (2020) Mechanisms, applications, and challenges of insect RNA interference. Ann Rev Entomol 65:293–311. https://doi.org/10.1146/annurev-ento-011019-025224
29. Ge XZ, Li Y, Gu S, Wang SS, Chao L, Cai WJ, Li HY, Fang YJ, Wang SG, Tang B (2023) Effects of *GLUT* gene expression on energy metabolism in *Harmonia axyridis*. Chin J Biol Control 39(1):98–110. https://doi.org/10.16409/j.cnki.2095-039x.2022.03.013
30. Livak KJ, Schmittgen TD (2001) Analysis of relative gene expression data using real-time quantitative PCR and the 2. method Methods 25(4):402–408. https://doi.org/10.1006/meth.2001.1262
31. Krasney PA, Carr C, Cavener DR (1990) Evolution of the glucose dehydrogenase gene in Drosophila. Mol Biol Evol 7(2):155–177. https://doi.org/10.1093/oxfordjournals.molbev.a040592
32. Zhang DW, Li Y, Zhang M, Wang SS, Xiao ZJ, Zeng BP, Ni XL, Tang B (2019) Expression and function of trehalase genes *TRE2-like* and *TRE2* during adult eclosion in *Harmonia axyridis* (Coleoptera: Coccinellidae). Acta Entomologica Sinica 62(6): 663–671. https://doi.org/10.16380/j.kcxb.2019.06.002
33. Arakane Y, Lomakin J, Gehrke SH, Hiromasa Y, Tomich JM, Muthukrishnan S, Beeman RW, Kramer KJ, Kanost MR (2012) Formation of rigid, non-flight forewings (elytra) of a beetle requires two major cuticular proteins. PLoS Genet 8(4):e1002682. https://doi.org/10.1371/journal.pgen.1002682
34. Rainio MJ, Margus A, Lehmann P, Helander M, Lindström L (2019) Effects of a glyphosate-based herbicide on survival and oxidative status of a non-target herbivore, the Colorado potato beetle (*Leptinotarsa decemlineata*). Comp Biochem Physiol C: Toxicol Pharmacol 215:47–55. https://doi.org/10.1016/j.cbpc.2018.09.005
35. Tang QH, Li WL, Wang JP, Li XJ, Li D, Cao Z, Huang Q, Li JL, Zhang J, Wang ZW, Guo J, Li JL (2023) Effects of spinetoram and glyphosate on physiological biomarkers and gut microbes in *Bombus terrestris*. Front Physiol 13:1054742. https://doi.org/10.3389/fphys.2022.1054742
36. Ning BY, Wang HL, Sun JX, Zhao TJ, Chang YQ, Zhan YY (2024) Expression of *GDH* gene and regulation mechanism of the *GDH* gene function by *HIF-1α* gene in sea urchin (*Strongylocentrotus intermedius*). J Dalian Ocean Univ 39(6):926–937. https://doi.org/10.16535/j.cnki.dlhyxb.2024-057
37. Cavener DR (1985) Coevolution of the glucose dehydrogenase gene and the ejaculatory duct in the genus Drosophila. Mol Biol Evol 2(2):141–149.

https://doi.org/10.1093/oxfordjournals.molbev.a040344

Figures

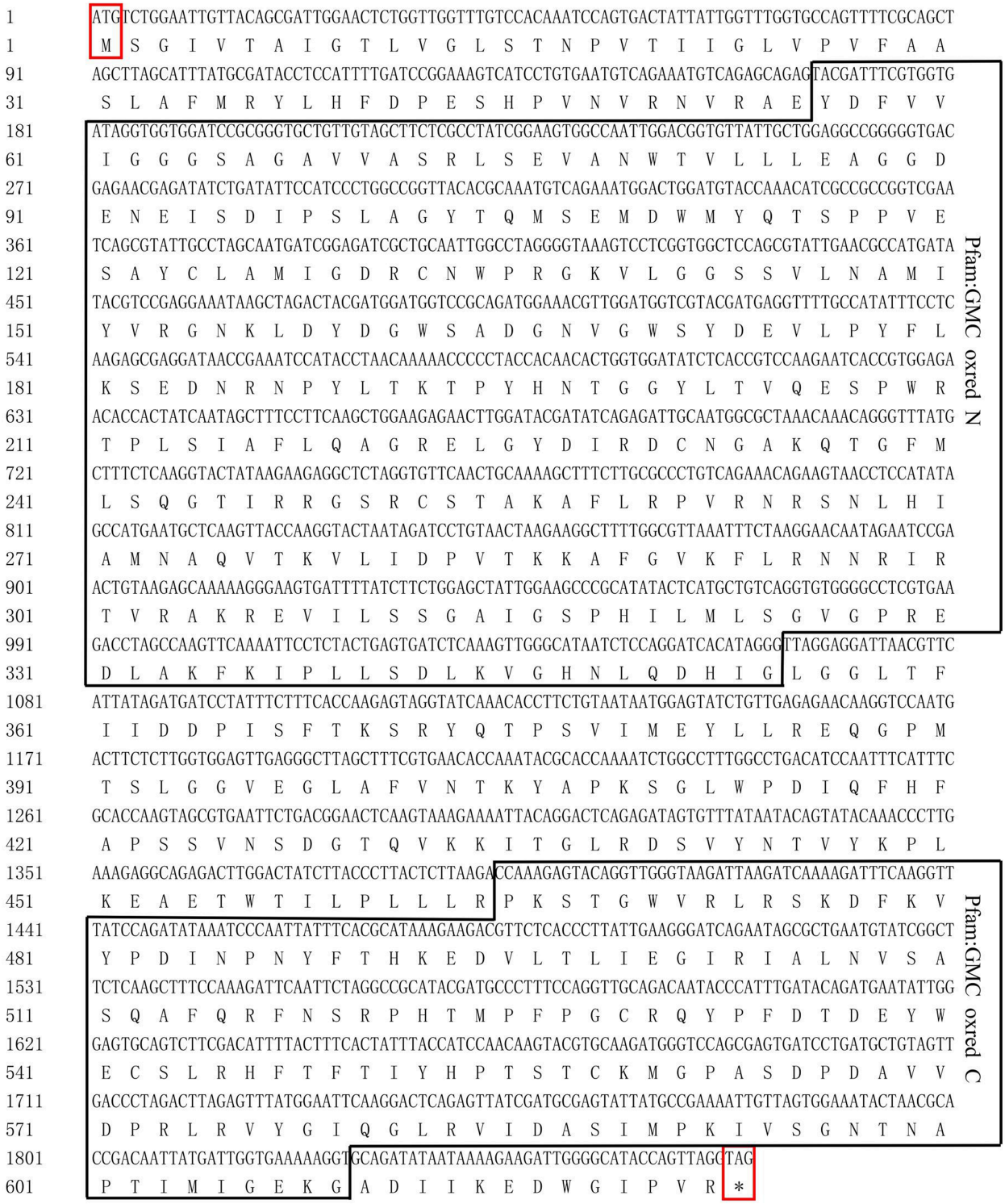


Figure 1

Nucleotide and putative amino acid sequence of the gene *HaGDH*

Note: The start codon (ATG) and stop codon (TGA) are enclosed in red boxes, and the stop codon is additionally marked with an asterisk. Functional domains are indicated by black boxes.

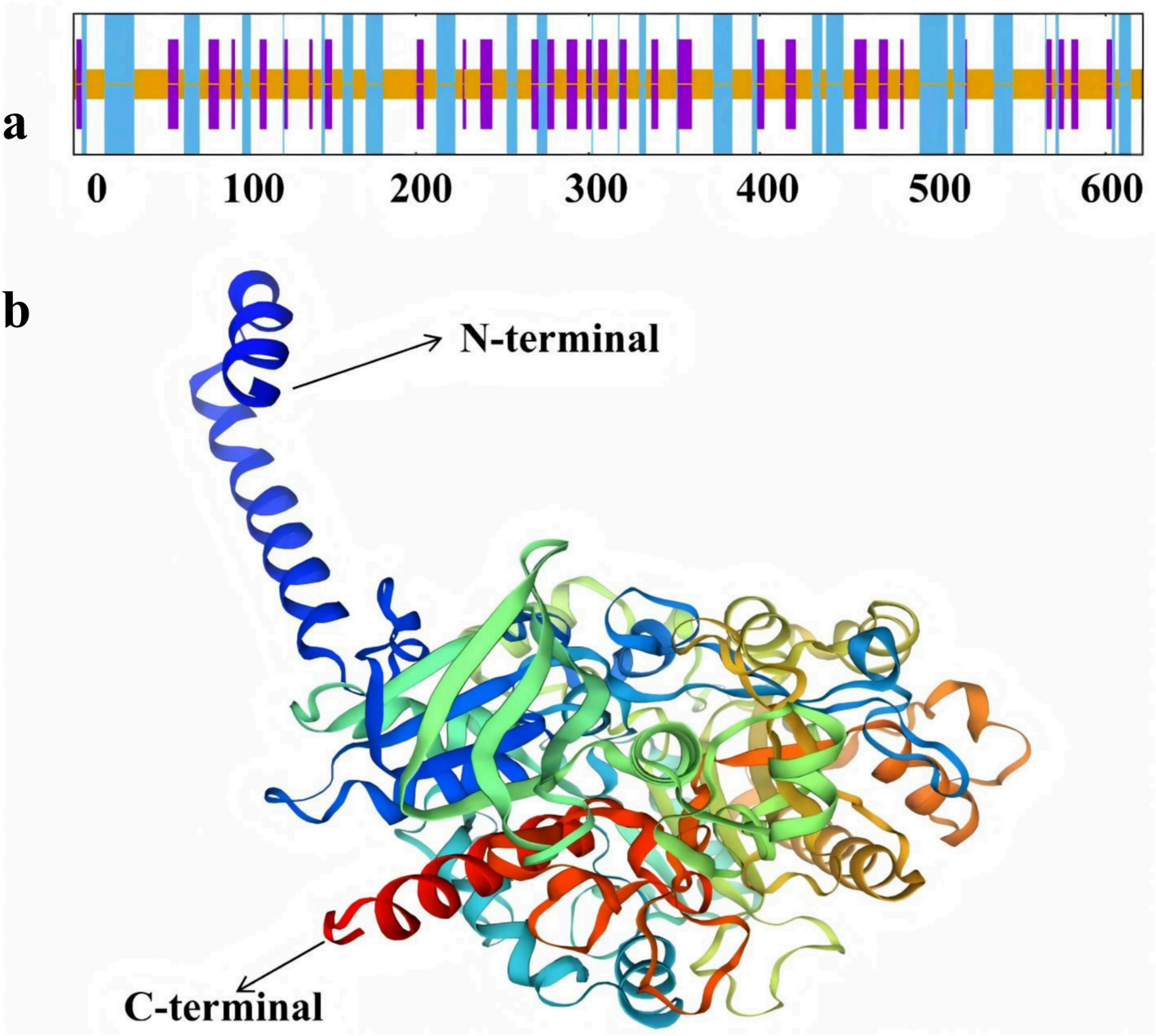


Figure 2

Prediction of secondary (a) (Blue line: α-helix Orange-yellow line: extended strand) and tertiary (b) structures of HaGDH proteins.

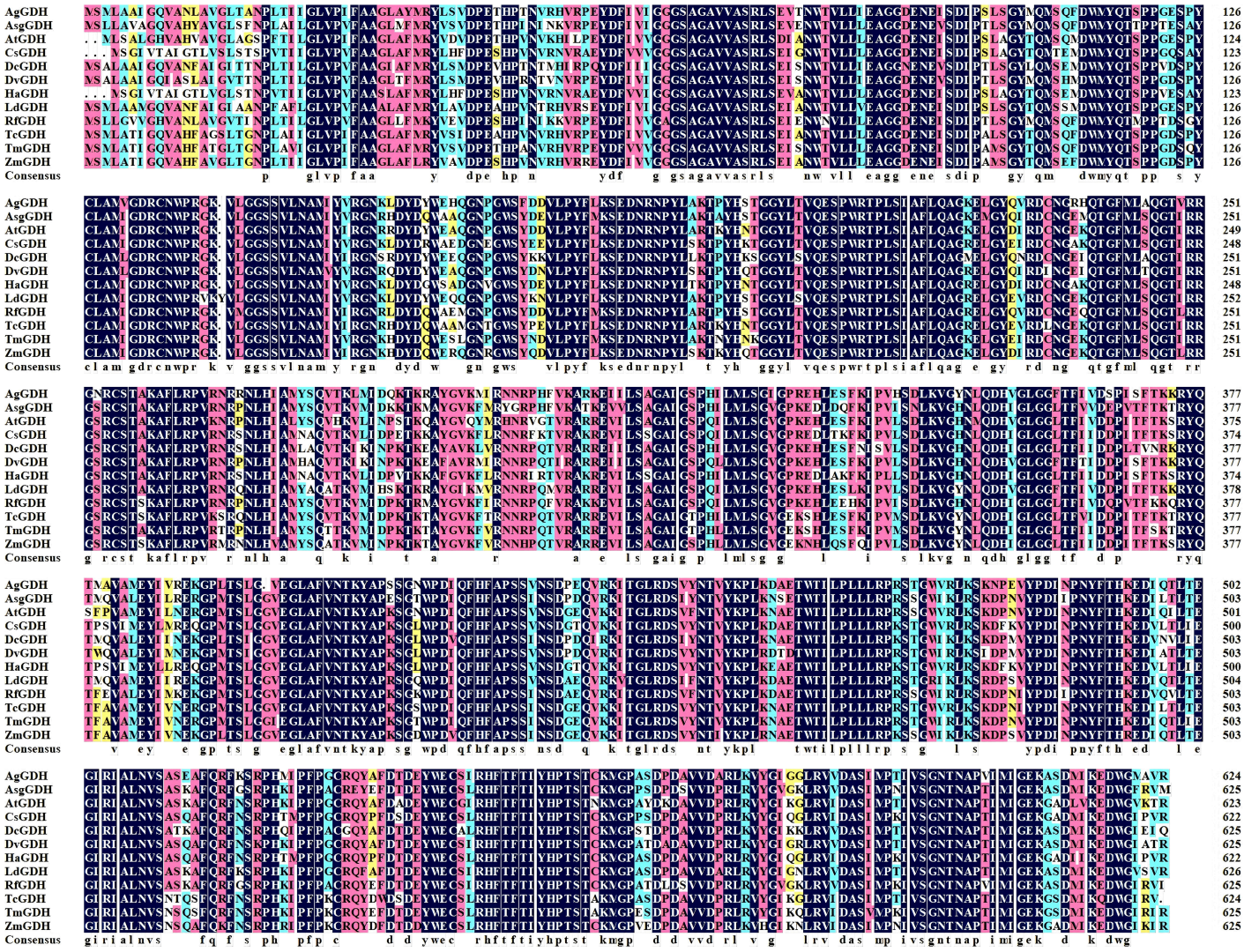


Figure 3

Multiple comparisons of the amino acid sequences of HaGDH and other insect GDHs.

(Note: The similarity between black and blue background coloration is 100%; that between purple and red background coloration ranges from 100% to 75%; for light blue background coloration, similarity ranges from 75% to 50%; and for yellow background coloration, similarity is 33%. Sequence information is sourced from NCBI, with the following accession numbers:AgGDH: *Anoplophora glabripennis* XP_018569543.1, AsgGDH: *Anthonomus grandis grandis* XP_050302397.1, AtGDH: *Aethina tumida* XP_019869157.2, CsGDH: *Coccinella septempunctata*XP_044763975.1, DcGDH: *Diorhabda carinulata* XP_057669065.1, DvGDH: *Diabrotica virgifera virgifera* XP_028134088.1, HaGDH: *Harmonia axyridis* , PZ594815.1, LdGDH: *Leptinotarsa decemlineata* XP_074030305.1, RfGDH: *Rhynchophorus ferrugineus* XP_076256267.1, TcGDH: *Tribolium castaneum* XP_972430.2, TmGDH: *Tenebrio molitor* XP_068900342.1, ZmGDH: *Zophobas morio*XP_063930047.1)



Figure 4

Phylogenetic tree of HaGDH and its homologous proteins constructed by the maximum-likelihood method. Note: The values at the branch nodes represent the confidence level of clustering based on 1000 bootstrap replicates, and the dots denote HaGDH from *H. axyridis*.

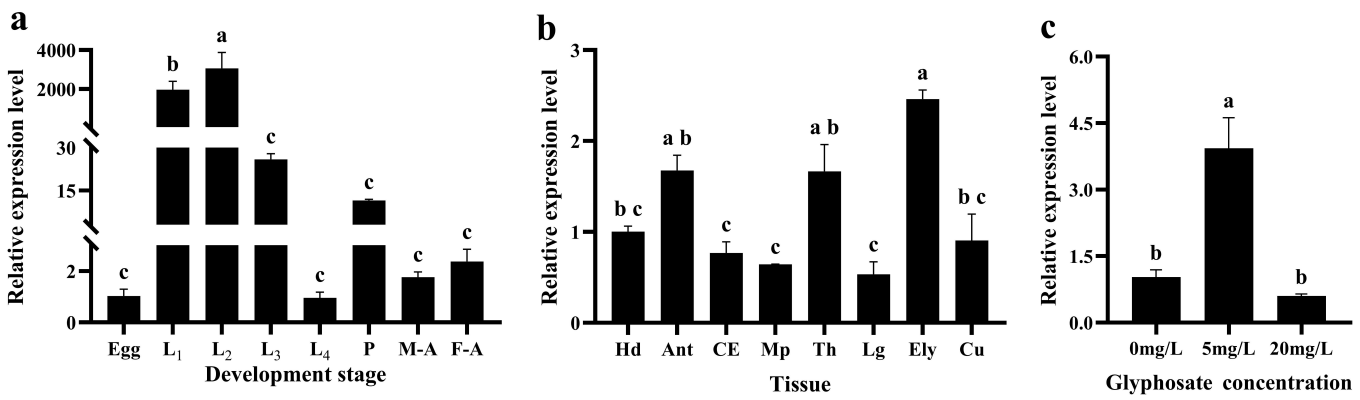


Figure 5

Expression levels of the *HaGDH* gene of *H. axyridis* at different developmental stages(a), in different tissues (b), and after Glyphosate stress(c). The values are means ± SE, and there was a significant difference between the relative expression of *HaGDH* (expressed by different lowercase letters). (Egg: Eggs; P: Pupae; MA: Male adults; FA: Female adults; Hd: Head; Ant: Antennae; CE: Compound eyes; Mp: Malpighian tubules; Th: Thorax; Ely: Elytra; Cu: Cuticula)

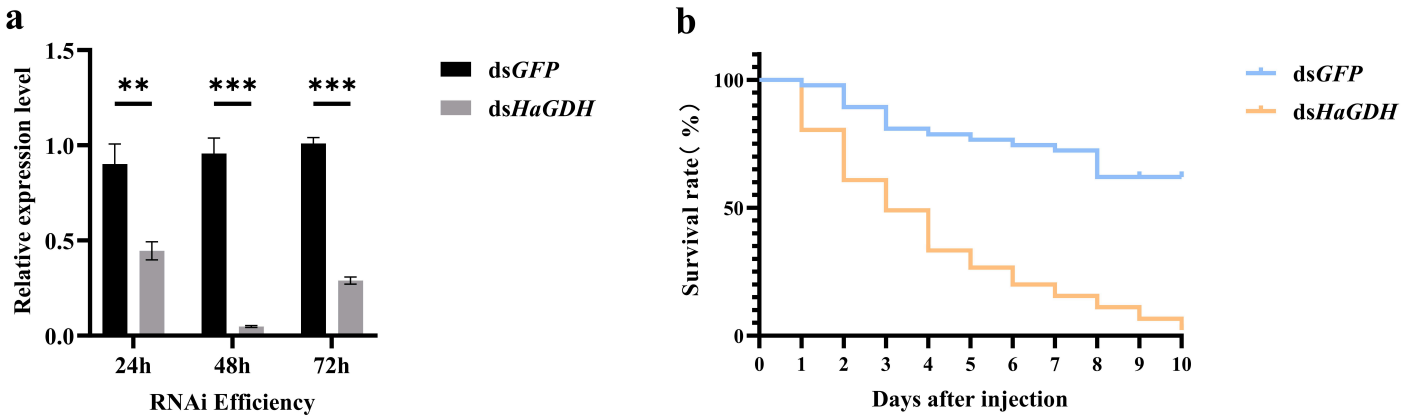


Figure 6

Expression level of *HaGDH* after dsRNA injection (a) and survival rate (b) of *H. axyridis*. Asterisks above bars indicate significant differences in the mRNA expression among the control and treatments $P \leq 0.01$ (**) and $P \leq 0.001$ (***). Data are means ± SE, n = 3.

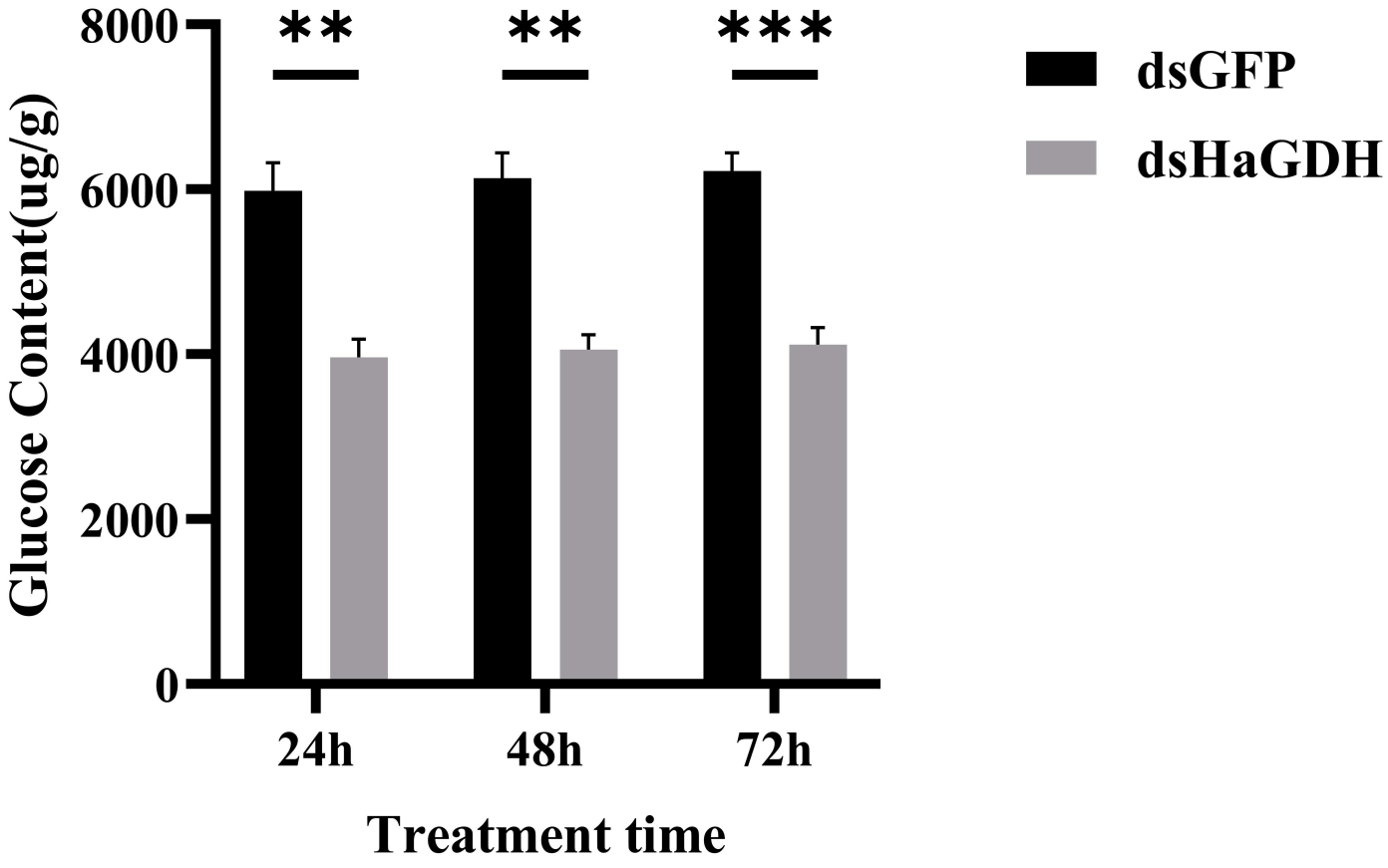


Figure 7

Glucose content in 4th-instar larvae of *H. axyridis* after *HaGDH* dsRNA injection (ds*HaGDH*). Asterisks above bars indicated significant differences in glucose content between the control and treatment groups $P \leq 0.01$ (**) and $P \leq 0.001$ (***). Data are means ± SE, n = 3.

Supplementary Files

This is a list of supplementary files associated with this preprint. Click to download.

- SupplementaryFig.S1.jpg
- SupplementaryFig.S2.jpg
- SupplementaryFig.S3.jpg